Available online at www.sciencedirect.com
ScienceDirect
Cement & Concrete Composites 28 (2006) 817–823
Cement & Concrete Composites
www.elsevier.com/locate/cemconcomp

Hydration characteristics of municipal solid waste incinerator bottom ash slag as a pozzolanic material for use in cement

K.L. Lin [a,*], D.F. Lin [b]

[a] Department of Environmental Engineering, National I-Lan University, I-Lan 260, Taiwan, ROC
[b] Department of Civil and Ecological Engineering, I-Shou University, Kaohsiung County 840, Taiwan, ROC

Received 17 October 2005; received in revised form 2 March 2006; accepted 30 March 2006
Available online 22 May 2006

Abstract

This study investigated the pozzolonic reactions and engineering properties of municipal solid waste incinerator (MSWI) bottom ash slag blended cements (SBC) with various replacement ratios. The 90-day compressive strengths developed by SBC pastes with 10% and 20% cement replacement by slags generated from the bottom ash were similar to that developed by ordinary Portland cement pastes. Thermal analyses indicated that the hydrates in the SBC pastes were mainly portlandite ($Ca(OH)_2$) and calcium silicate hydrate (C–S–H) gels, similar to those found in ordinary Portland cement paste. It is also indicated that the slag reacted with $Ca(OH)_2$ to form C–S–H. The average length (in terms of the number of Si molecules) of linear polysilicate anions in C–S–H gel, as determined by ^{29}Si nuclear magnetic resonance, increased in all the SBC pastes with increasing curing age, which outperformed that of ordinary Portland cement at 90 days. It can thus be concluded from the study results, that municipal solid waste incinerator bottom ash can be processed by melting to obtain reactive pozzolanic slag, which may be used in SBC to partially replace the cement.

Keywords: Portland cement; Melting process; Slag; Pozzolanic; C–S–H gel

1. Introduction

Incineration is expected to become a major municipal waste management alternative, as it is not only effective in terms of waste volume reduction, but can also produce benefits in terms of energy recovery. However, municipal solid waste incinerator ash is piling up at incinerator facilities in Taiwan and has became the source of other types of environmental problems. Ninety percent of the total amount is bottom ash and 10 percent is fly ash. Mineralogical studies have found that MSWI bottom ash is composed of equal amounts of fine ash material and small quantities of crystallized, metallic components, ceramics and stones [1]. Chimenos et al. have reported that the major components in bottom ash are SiO_2, CaO and Al_2O_3. The SiO_2 content increases as the particle size of the bottom ash increases, but the CaO increases as the particle size of bottom ash decreases [2]. Heavy metals are mainly found in the finer fraction [3].

About 50% or more of treated MSWI bottom ash is used as secondary building material or for similar purposes, such as for road beds, the construction of embankments, and other civil engineering applications [4–6]. Nevertheless, bottom ash is subject to chemical problems, which can induce expansion, which in turn brings about cracking, and finally road destruction [7].

The successful synthesis of such materials from MSWI fly ash has been done by melting, using slag as a raw material [8–10]. The use of vitrification treatment enables any heavy metals in the waste residues to become immobilized. The main constituents of the bottom ash are the glass network formers, SiO_2 and Al_2O_3, as well as the glass network

* Corresponding author. Tel.: +886 3 9357400x749; fax: +886 3 9359674.
E-mail address: kllin@niu.edu.tw (K.L. Lin).

0958-9465/$ - see front matter © 2006 Elsevier Ltd. All rights reserved.
doi:10.1016/j.cemconcomp.2006.03.003

modifiers, CaO and Na_2O. Thus by means of the thermal treatment, melting, and rapid cooling of the bottom ash, it is possible to form a glassy material. This work is aimed at studying the pozzolanic properties of MSWI bottom ash slag and ways to improve its reactivity.

2. Materials and methods

2.1. Materials

2.1.1. MSWI bottom ash

The bottom ash used in this study was collected from a mass-burning incinerator located in the northern part of Taiwan. Thermal treatment tests were performed with water-quenched bottom ash taken from a municipal solid waste incinerator. The ash was screened and magnetically separated to remove any coarse non-ferrous impurities and ferrous substances, then dried at 105 °C for 24 h.

2.1.2. Cement

The cement used in this research was ordinary Portland cement Type I (OPC), supplied by the Taiwan Cement Company.

2.1.3. Slag made from MSWI bottom ash

The MSWI bottom ash slag was prepared by melting the above bottom ash in a 20 l capacity electric-heated melter at 1400 °C for 30 min. The melts were water-quenched to obtain fine slag, which was then ground in a ball mill until fine enough to pass through a #200 sieve. The resultant pulverized slag had a specific surface of approximately 500 m^2/kg, with a specific gravity ranging from 2.7 to 2.9, close to that of ordinary Portland cement.

2.1.4. Preparation of specimens of slag blended cement paste

SBC pastes were mixed homogeneously with cement, slag made from MSWI bottom ash, and water, in a mixer. The substitution levels of slag in the blended cement were between 10% and 40%. The water/binder (w/b) ratio of SBC paste was constant, 0.38. The pozzolanic activity index of the SBC pastes was determined according to ASTM C311. SBC paste cubes were prepared, according to ASTM C109, by pouring the paste into rectangular molds, which remained under ambient conditions for 24 h, after which they were demolded, and finally cured in an environmental chamber maintained at 25 °C, with a relative humidity > 98%, for periods ranging from 1 day to 90 days. After curing for 1, 3, 7, 14, 28, 60 or 90 days, the SBC paste cubes were subjected to unconfined compressive strength tests. Subsequently, the hydration reactions crushed samples were terminated with methyl alcohol. They were then subjected to X-ray diffraction (XRD), differential thermal and thermogravimetric analysis (DTA/TGA) and nuclear magnetic resonance (NMR) analyses.

2.2. Analytical methodology

The major analyses performed on the SBC paste and its cubes included compressive strength, toxicity characteristic leaching procedure and chemical composition tests.

2.2.1. Toxicity characteristic leaching procedure (TCLP): SW 846-1311

This extraction procedure requires the preliminary evaluation of the pH characteristics of the sample, to determine the proper extraction fluid necessary for the experiments. It was determined after testing that #B extraction fluid (pH 2.88 ± 0.05) should be used for the TCLP analysis. This fluid was prepared by adding 5.7 ml of acid to 500 ml of double distilled water, diluted to a volume of 1 l. A 25 g sample was placed in a 1 l Erlenmeyer flask after which 500 ml of extraction fluid were added to each Erlenmeyer flask. The samples were agitated for 18 h using an electric vibrator. The slurry was filtered with 6–8 μm pore size Millipore filter paper. The leachates were preserved in 2% HNO_3.

2.2.2. X-ray diffraction analysis

The XRD analysis was carried out by a Siemens D-5000X-ray diffractometer with CuKα radiation and 2θ scanning, ranging between 5° and 70°. The XRD scans were run at 0.05° steps, with a 1 s counting time.

2.2.3. DTA/TGA analysis

DTA/TGA analysis of the samples was performed using a Seiko SSC Model 5000 thermal analyzer. Dry N_2 gas was used as the stripping gas. The heating rate was 0.5 °C. The samples were heated from 50 to 1000 °C.

2.2.4. Chemical shift of linear polysilicate anions in C–S–H by ^{29}Si MAS/NMR (^{29}Si magnetic angle spinning/nuclear magnetic resonance)

The degree of hydration of the main constituents of the clinkers, the C_2S and the C_3S, and the average length of the linear polysilicate anions in the calcium silicate hydrate (C–S–H) gels, which are primarily responsible for the strength development, were analyzed by using high-resolution solid-state ^{29}Si MAS/NMR techniques. As a result of the degree of increasing condensation, there was an increase of diamagnetic shielding to the ^{29}Si nuclei, from the single tetrahedral structure of the monosilicates (Q^0) to the end groups (Q^1), to the chain middle groups (Q^2), to the layers and the

Table 1
Range of ^{29}Si chemical shifts of Q^n units in solid silicates

Type	Symbol	Range (ppm)
Monosilicates	Q^0	−68 to −76
Disilicates and chain end group	Q^1	−76 to −82
Chain middle groups	Q^2	−82 to −88
Chain branching sites	Q^3	−88 to −92
Three-dimensional network	Q^4	−92 to −129

Table 2
Chemical composition of OPC, bottom ash and slag

	SiO_2 (%)	CaO (%)	Al_2O_3 (%)	Fe_2O_3 (%)	Na_2O (%)	K_2O (%)	MgO (%)	SO_3 (%)	pH
OPC	20.5	62.5	6.5	3.2	<0.01	<0.01	0.95	<0.01	–
Bottom ash	25.6	26.1	6.33	10.33	3.92	1.13	0.82	0.47	12.2
Slag	31.07	26.44	8.87	11.21	2.39	0.92	1.4	0.09	9.6

branching sites (Q^3), and finally to the three-dimensional networks (Q^4), which led to well-separated, analytically useful chemical shift ranges for each type of SiO_4^{4-} unit. In other words, the calcium silicate hydrates, that is the hydration products in cement, can be semi-quantified using chemical shifts in the ^{29}Si nuclei in Si–O–X groups, whose structures are shown below:

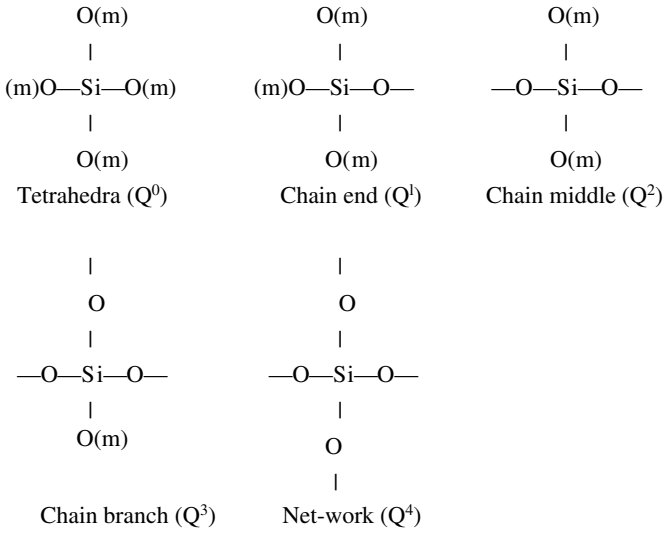

High-resolution ^{29}Si MAS/NMR spectra were recorded at 39.72 MHz on an MSL Bruker MAS/NMR-200 solid-state high-resolution spectrometer, using rapid (about 3 kHz) sample spinning at the magic angle to the external magnetic field. The ^{29}Si chemical shifts are given relative to the primary standard liquid tetramethylsilane (TMS) in the delta-scale (the negative signs correspond to up-field shifts). The sharp ^{29}Si signal chemical shifts for the above Si–O–X groups in solid silicates are summarized in Table 1.

The degree of hydration (α) of the main constituents of the clinkers, C_2S and C_3S, can be calculated as follows:

$$\alpha(\%) = \left[1 - \frac{I(Q^0)}{I^0(Q^0)}\right] \times 100\% \quad (1)$$

where $I^0(Q^0)$ and $I(Q^0)$ represent the integral intensity of the hydrated cement paste and the cement powder at -70 ppm (Q^0), respectively.

Similarly, the average length of linear polysilicate anions in calcium silicate hydrates (C–S–H gels) can be evaluated by

$$\Psi = 2\left[1 + \frac{I(Q^2)}{I(Q^1)}\right] \quad (2)$$

where Ψ is the average length of linear polysilicate anions in calcium silicate hydrates; $I(Q^1)$ and $I(Q^2)$ represent the

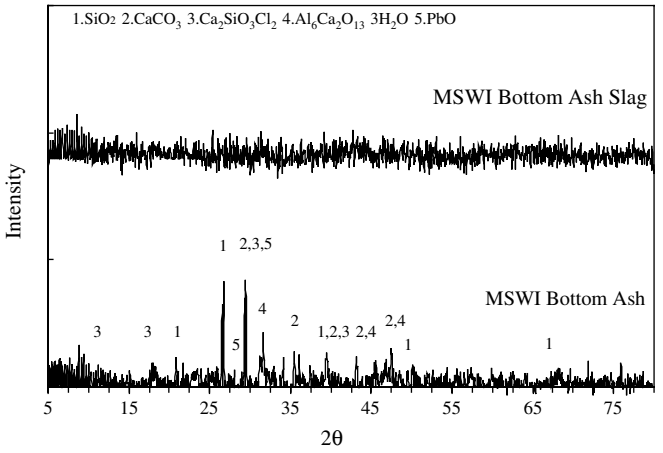

Fig. 1. XRD pattern of MSWI bottom ash and slag.

Table 3
Total metal and TCLP leaching concentrations for MSWI bottom ash and slag

	Pb	Cd	Cr[a]	Cu	Zn
Total metal (mg/kg)					
Bottom ash	5195 ± 33.2	27 ± 0.6	276 ± 12.4	432 ± 47.9	8352 ± 184.0
Slag	609.4 ± 7.24	5.3 ± 0.03	1719.3 ± 9.77	136.3 ± 4.84	4949.6 ± 17.79
TCLP (mg/l)					
Bottom ash	0.59 ± 0.05	0.24 ± 0.01	0.26 ± 0.01	5.49 ± 0.03	0.18 ± 0.08
Slag	0.35 ± 0.03	0.17 ± 0.01	ND	0.19 ± 0.01	120.34 ± 1.41
Taiwan regulatory limits	5.0	1.0	5.0	15	–

[a] Cr detection limits <0.016 mg/l.

integral intensity of the signals at −80 ppm (Q^1) and −87 ppm (Q^2), respectively.

3. Results and discussion

3.1. Characterization of MSWI bottom ash and slag

Table 2 lists the major components of the MSWI bottom ash and slag used in this study. The major components in the ash are shown in Table 2, with SiO_2, CaO, Fe_2O_3 and Al_2O_3 comprising 25.6 wt.%, 26.1 wt.%, 10.3 wt.% and 9.8 wt.%, respectively. The next most abundant components are Na_2O, K_2O and MgO, contributing about 3.9 wt.%, 1.1 wt.% and 0.8 wt.% each. The ash (defined as CaO/SiO_2) has a basicity of 1.02 and a pouring point of approximately 1310 °C. Identification of the various crystalline phases was achieved through reference to diffraction patterns provided by Joint Committee on Powder Diffraction Stansard (JCPDS). SiO_2, $CaCO_3$, Ca_2SiO_3Cl and $Al_6Ca_2O_{13} \cdot H_2O$ were identified by X-ray diffraction analysis of the MSWI bottom ash were shown in Fig. 1.

The slag was composed of SiO_2 (25.6 wt.%), CaO (26.1 wt.%) and Al_2O_3 (6.3 wt.%), and had a Pozzolanic activity index of 91.8. The X-ray diffraction pattern of the MSWI bottom ash slag was shown in Fig 1. As can be seen, the slag contained large amounts of glass, indicated by the broad diffuse bands between 10–15 and 25–35° (2θ).

The TCLP leaching concentrations of the target metals in the MSWI bottom ash slag all met the Taiwan EPA's current regulatory thresholds (Table 3), indicating that the heavy metals had been immobilized in the vitrified product, making then highly resistant to leaching.

3.2. Development of compressive strength

The compressive strength results are given in Fig. 2. In the first 7 days, the use of the slag lowered the strength

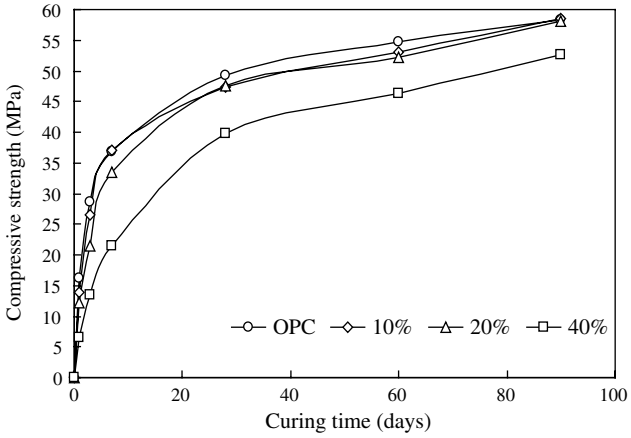

Fig. 2. Compressive strength of MSWI bottom ash slag blended cement pastes.

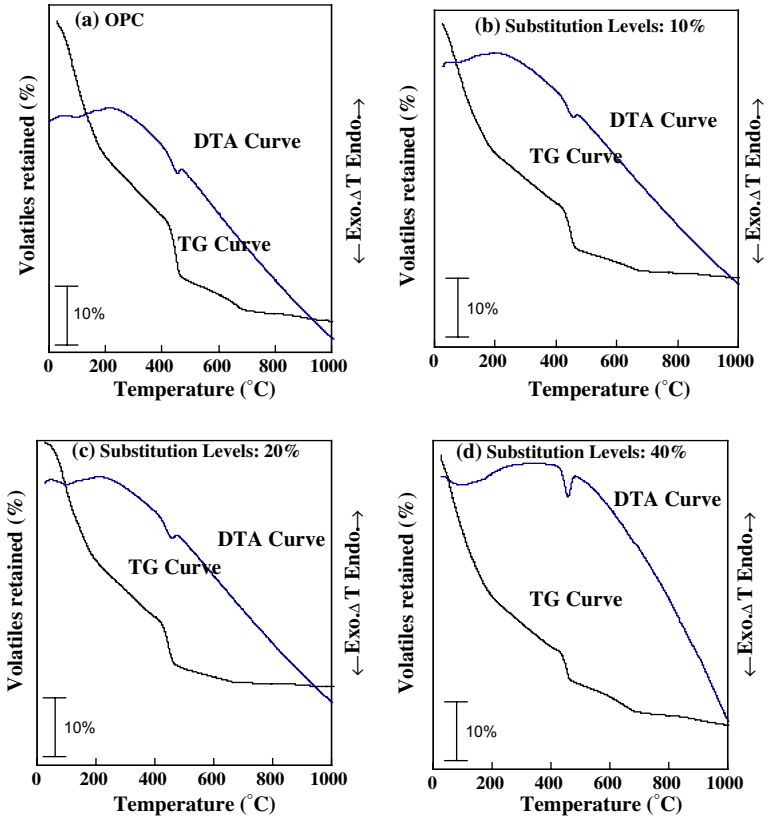

Fig. 3. Differential thermal and thermogravimetric analysis of OPC and SBC pastes with different substitution levels. (a) 0%, (b) 10%, (c) 20% and (d) 40%.

of the paste, as shown in Fig. 2. The results also indicate that the cementitious reactions of the slag tended to retard the cementitious reactions during the early stages. This may be due to reactions in the slag, which consumed part of the calcium hydroxide formed during the earlier stages of hydration. However, at a later stage (28–90 days), the Compressive strength of SBC paste samples containing 10% and 20% substitution levels of slag varied from 95% to 100% of that developed by the plain Portland cement paste (Fig. 2). The MSWI bottom ash slag was activated by the calcium hydroxide produced during the hydration of the Portland cement clinkers.

Even in SBC paste samples containing 40% substitution levels of slag, the compressive strengths at the early and later stages were all less than the plain Portland cement paste. The compressive strength development by the 40% substitution levels of slag, at 7, 28 and 90 days, exhibited a decline in the compressive strength, by 58%, 81%, and 90%, respectively, compared to that developed by the plain cement paste.

3.3. Differential thermal and thermogravimetric analysis SBC pastes

Thermal data for the hydration products of both OPC and MSWIBA slag pastes after 28 days can be seen in Fig. 3. The DTA curves for the OPC pastes cured from 1 to 90 days show two endothermic effects, at 100–200 and 400–480 °C (Fig. 2). The endotherms observed in the DTA curves in the temperature regions of 100–200 °C, accompanied by breaks in the TG curves are due to the presence of C–S–H, C–A–S–H gels, gehlinite hydrates and hydrogarnets (C_3AH_6) [11,12]. The endotherms in the DTA curves at the temperature ranges from 400 to 480 °C, accompanied by weight loss, as exhibited by the corresponding TG curves, are due to the dehydroxylation of $Ca(OH)_2$. The hypothesis is that OPC hydrates via the liberation of $Ca(OH)_2$. The $Ca(OH)_2$ reacts with the active silica constituents in the MSWI bottom ash slag to form C–S–H. The second peak can be attributed to the decomposition of $Ca(OH)_2$. Table 4 indicates that as the hydration proceeds up to 90 days, the amount of C–S–H increases. It can be seen that OPC becomes hydrated by producing $Ca(OH)_2$, which increases over time up to 28 days, then decreases up to 90 days.

Fig. 3(b)–(d) show the results of the thermogravimetric analysis of SBC paste samples containing 10%, 20% and 40% substitution levels of slag, respectively. It also illustrates the endothermic effects at 100–200 and 400–480 °C.

On the other hand, it can be seen that $Ca(OH)_2$ is formed in smaller amounts than for the OPC pastes. As hydration proceeds, the amount of C–S–H gel at 400–480 °C increases with time. Table 4 indicates that the SBC paste samples containing 10% and 20% substitution levels of slag have lower C–S–H values than do the OPC pastes, at 28 days of hydration. However, at a later stage (90 days), the SBC pastes samples containing 10% and 20% substitution levels of slag have higher CSH values than do the pure OPC pastes. This may be due to the reactions in the slag, which consumed part of the calcium hydroxide and formed C–S–H gels. It is indicated that hydration and pozzolanic reactions continued. The SBC pastes samples containing 40% substitution levels of slag had lower C–S–H and $Ca(OH)_2$ values than did the OPC pastes, at all stages of hydration.

Table 4
C–S–H and $Ca(OH)_2$ amounts in the OPC and SBC pastes

Curing time (days)	Hydration products (%)	Substitution levels (%)			
		OPC	10%	20%	40%
28	C–S–H	16.62	16.88	15.90	14.41
28	$Ca(OH)_2$	4.67	4.23	3.78	4.04
90	C–S–H	17.18	19.19	18.02	13.55
90	$Ca(OH)_2$	6.34	5.54	4.77	4.49

3.4. ^{29}Si NMR spectra of hydrated SBC pastes

Figs. 4 and 5 show the spectra for OPC and SBC pastes containing 20% substitution levels of slag, respectively. The chemical shift of ^{29}Si nuclei in various silica materials is

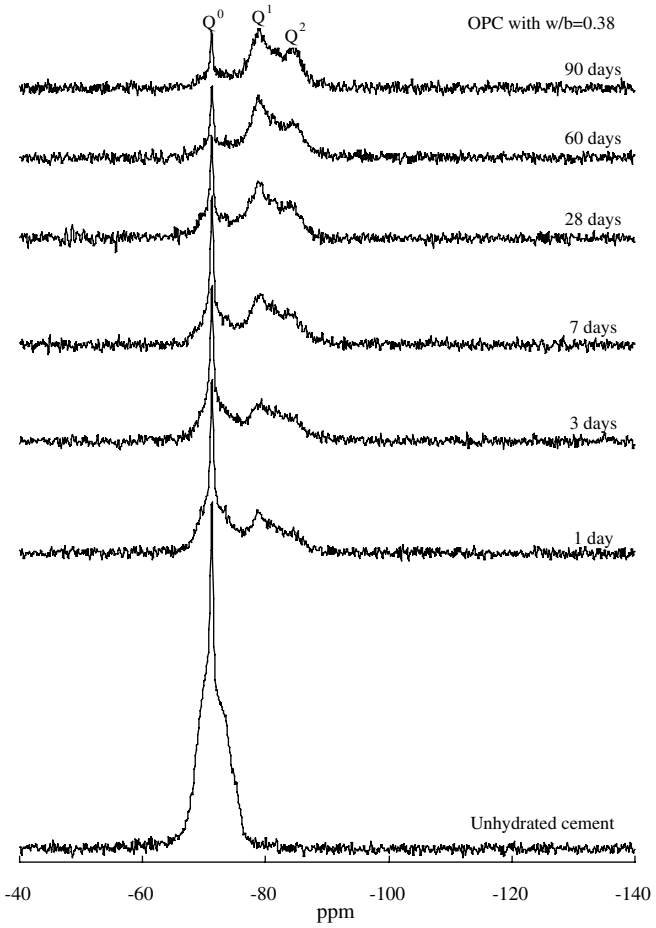

Fig. 4. ^{29}Si NMR spectrum of Portland cement pastes samples.

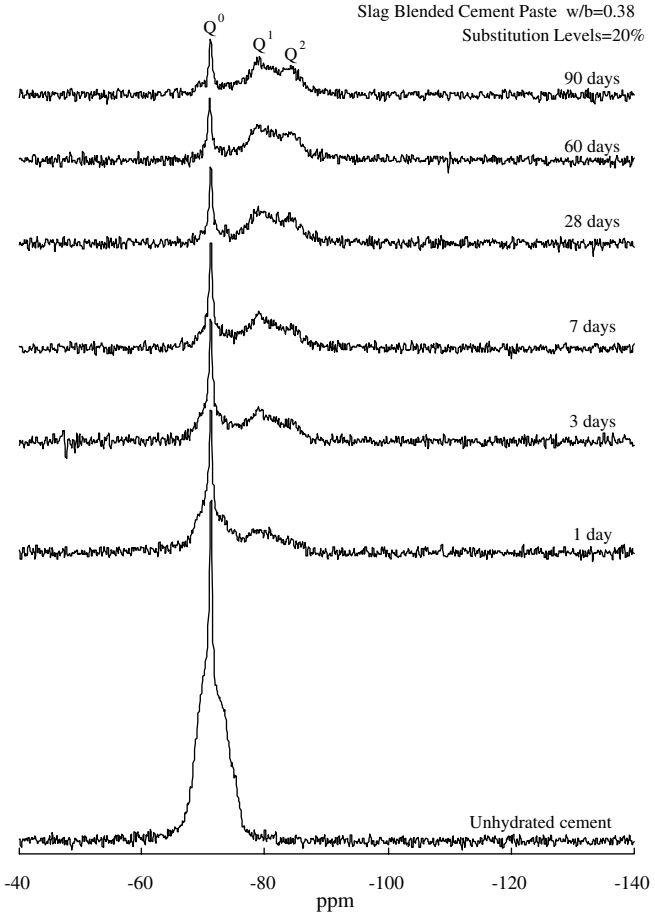

Fig. 5. ^{29}Si NMR spectrum of hydrated slag blended cement pastes samples containing 20% substitution levels of slag.

dependent on the X-group in the Si–O–X units. The orthosilicate unit SiO_4^{4-} (designated as Q^0), in Portland cement reacts, with water to produce siliceous polymers. The figure shows the unhydrated spectrum, with a main peak at −71 ppm (Q^0) and a pronounced shoulder at −73 ppm; this structure is due to the contributions of C_2S and C_3S, while the peaks corresponding to −79 and −84 ppm indicate the Q^1 and Q^2 peaks, respectively. No evidence can be seen in this sample of Q^3 and Q^4 peaks.

Fig. 5 shows the spectrum for hydrated slag blended cement pastes samples containing 20% substitution levels of slag. There are two peaks and a pronounced shoulders at −71, −79 and −84 ppm, respectively. Furthermore, the peak for the Q^0 group decreased, while the Q^1 and Q^2 hydrate peaks increased, with increasing curing time. The ^{29}Si NMR spectra of hydrated SBC pastes shows that about 33.4% of the silicate is still in the Q^0, some 35.8% is in the Q^1 state, and 30.7% is in the Q^2 state, after 90 days of curing. The incorporation of slag-derived Si and Al in the hydration products will influence the resulting peak intensities from which chain length calculations have been made. The degree of hydration, as well as the average length (in terms of the Si number) of linear polysilicate anions in the C–S–H gel, were calculated and the results

Table 5
^{29}Si NMR analysis for slag blended monoliths cured for different age

Sample	^{29}Si NMR integral intensities of Q^n (mm^2)					Degree of hydration (%)	Average length of linear polysilicate anions
	Q^0	Q^1	Q^2	Q^3	Q^4		
OPC							
1 day	582	261	157	–	–	31.5	3.206
3 days	543	280	177	–	–	36.1	3.266
7 days	465	321	214	–	–	45.3	3.332
28 days	406	355	239	–	–	52.3	3.344
60 days	323	402	275	–	–	62.0	3.366
90 days	310	405	285	–	–	63.5	3.406
Substitution levels (10%)							
28 days	407	351	243	–	–	52.1	3.385
90 days	313	389	298	–	–	63.2	3.532
Substitution levels (20%)							
1 day	666	214	120	–	–	21.6	3.120
3 days	537	285	177	–	–	36.8	3.244
7 days	469	324	207	–	–	44.8	3.278
28 days	375	359	266	–	–	55.8	3.480
60 days	359	355	287	–	–	57.8	3.617
90 days	334	358	307	–	–	60.7	3.716
Substitution levels (40%)							
28 days	353	345	302	–	–	58.4	3.753
90 days	361	320	319	–	–	57.5	3.991

are summarized in Table 5. Both the degree of hydration and the average polysilicate length of the hydrated SBC paste show a tendency to increase with the curing time.

4. Conclusions

The effects of cement replacement by slag (prepared by melting MSWI bottom ash) on the pozzolanic reactivity of SBC paste was investigated. The slag contained large amounts of glass, in which any heavy metals were immobilized in the vitrified product, making then highly resistant to leaching.

The results suggest that the early strength of the tested pastes decreased as the replacement levels increased for pastes with substitution levels less than 20%, whereas the later strength showed typical SBC properties, similar to the OPC paste.

The development of later strength was also suggested by the DTA/TGA techniques, implying that the active amorphous ions (Si, Al) reacted with the hydration products, $Ca(OH)_2$, to form C–S–H, increasing the averaged length of linear polysilicate anions in the C–S–H gel, which in turn contributed to the later strength. Thus pozzolanic reactivity in the SBC pastes make it possible for them to be used as a substitute for OPC in blended cement.

References

[1] Johnson A, Brandenberger S, Peter B. Acid neutralizing capacity of municipal waste incinerator bottom ash. Environ Sci Technol 1995;29:142–7.

[2] Chimenos JM, Fernandez MA, Espiell F. Characterization of the bottom ash in municipal solid waste incineration. J Hazard Mater 1999;A64:211–22.
[3] International Ash Working Group (AWG). Municipal solid waste incinerator residues. Studies environmental science, vol. 67. Amsterdam: Elsevier Science BV; 1997.
[4] Hjelmar O. Disposal strategies for municipal solid waste incineration residues. J Hazard Mater 1996;47:345–68.
[5] Wiles CC. Municipal solid waste combustion ash: sate-of-the-knowledge. J Hazard Mater 1996;47:325–44.
[6] Chimenos JM, Segarra M, Fernandez MA, Espiell F. Short-term natural weathering of MSWI bottom ash. J Hazard Mater 2000;B79:287–99.
[7] Pecqueur G, Crignon C, Quenene B. Behaviour of cement-treated MSWI bottom ash. Waste Manage 2001;21:229–33.
[8] Lin KL, Wang KS, Tzeng BY, Lin CY. The reuse of municipal solid waste incinerator fly ash slag as a cement substitute. Res Conserv Rec 2003;39(4):315–24.
[9] Lin KL, Wang KS, Tzeng BY, Lin CY. Hydraulic activity of slag obtained by vitrification of the MSWI fly ash. Waste Manage Res 2003;21:567–74.
[10] Wang KS, Lin KL, Tzeng BY. Latent hydraulic reactivity of blended cement incorporating slag made from municipal solid waste incinerator fly ash. J Air Waste Manage Assoc 2003;53:1340–6.
[11] De-Silva PS, Glasser FP. Phase relation in the system $CaO–Al_2O_3–SiO_2–H_2O$ relevant to metakaolin–$Ca(OH)_2$ hydration. Cem Concr Res 1993;23:627–39.
[12] Serry MA, Taha AS, El-Jemaly SAS, El-Didamony H. Metakaolin–lime hydration products. Therm Chim Acta 1984;79:103–10.